frontiers | Frontiers in Water

TYPE Original Research
PUBLISHED 25 October 2023
DOI 10.3389/frwa.2023.1255495

OPEN ACCESS

EDITED BY
Bhavna Arora,
Berkeley Lab (DOE), United States

REVIEWED BY
Wei Shao,
Nanjing University of Information Science and Technology, China
Ty Ferre,
University of Arizona, United States
Dhruva Kathuria,
Goddard Earth Sciences Technology and Research (GESTAR), United States

*CORRESPONDENCE
Yasmin Mbarki
✉ Yasmin.mbarki.1@ulaval.ca

RECEIVED 08 July 2023
ACCEPTED 03 October 2023
PUBLISHED 25 October 2023

CITATION
Mbarki Y, Gumiere SJ, Celicourt P and Brédy J (2023) Study of the effect of the compaction level on the hydrodynamic properties of loamy sand soil in an agricultural context. *Front. Water* 5:1255495. doi: 10.3389/frwa.2023.1255495

Study of the effect of the compaction level on the hydrodynamic properties of loamy sand soil in an agricultural context

Yasmin Mbarki[1]*, Silvio José Gumiere[1], Paul Celicourt[2] and Jhemson Brédy[1]

[1]Faculté des Sciences de l'Agriculture et de l'Alimentation, Université Laval, Québec, QC, Canada, [2]Unité Mixte de Recherche INRS-UQAR, Centre Eau Terre Environnement, Institut National de la Recherche Scientifique, Rimouski, QC, Canada

Agricultural soil compaction adversely affects crop water use and yield performance and should be avoided or remediated through appropriate soil management strategies. The investigation of the impact of different levels of soil compaction on its hydrodynamic properties remains a crucial step in improving water use and crop yields. We examined five compaction levels of silty sand soil sampled from a potato field in the agricultural regions of northern Quebec (Canada). Soil hydraulic characteristics (saturated and unsaturated hydraulic conductivity, soil water retention capacity) were measured using the constant head method, the HYPROP device, and a WP4C dew point potentiometer. The sixteen hydraulic models integrated into the HYPROP software were fitted to the soil water retention curve (SWRC) data for the studied compaction levels. Statistical parameters such as the mean bias error, mean absolute error, correlation coefficient, and root mean square error were used to measure the performance of the models. The results show that saturated and unsaturated conductivity decreases with increasing soil compaction. The lowest saturated hydraulic conductivity (Ks) value is observed for the highest level of soil compaction, reflecting a solid medium with less pore space and connectivity. Among the hydraulic models, the Peters-Durner-Iden (PDI) variant of van Genuchten's unconstrained bimodal model (VGm-b-PDI) outperformed all other models for SWRC simulation of different soil compaction levels and was, accordingly, selected as the optimal model. This model was implemented in HYDRUS-1D to estimate the amount of irrigation for different compaction levels. We simulated irrigation scenarios with the dual-porosity model. The results indicated that soil compaction can strongly influence soil hydraulic properties and water differently. However, the amount of irrigation for the potato crop was optimal at a moderate level of soil compaction. Overall, combined HYPROP and HYDRUS 1D can provide helpful information on the soil hydraulics properties dynamics and a rigorous simulation for irrigation planning and management in potato fields.

KEYWORDS

soil compaction, soil water retention curve (SWRC), hydraulic conductivity, HYPROP, WP4C, HYDRUS-1D

1. Highlights

This article focuses on the effect of compaction on soil water retention and hydraulic conductivity functions.

- The effect of the compaction levels of loamy sand soil on the water retention curve and unsaturated hydraulic conductivity curve was investigated.
- The joint HYPROP and WP4C system were used to determine the soil hydraulic properties.
- The PDI bimodal van Genuchten model yielded excellent SWRC results.
- The constrained PDI van Genuchten model best reflected the unsaturated hydraulic conductivity.
- The amount of irrigation was optimal for the potato crop with a moderate compaction level using the dual porosity model in the HYDRUS-1D software.

2. Introduction

Soil compaction represents a significant concern for farmers in many regions of the world (Jabro et al., 2021). Agricultural management practices, wheeled vehicle and equipment traffic over cropland increase soil compaction, and negatively affect its hydraulic properties. Consequently, about 68.3 million hectares of soil have been affected worldwide (Nawaz et al., 2013). Increased soil bulk density from compaction reduces root growth which may result in crop yields reduction by up to 50% depending on the soil depth (Sidhu and Duiker, 2006). Compaction also affects pore geometry (Matthews et al., 2010), it alters soil basic hydrological properties such as water retention and hydraulic conductivity. According to Filipović et al. (2021), the soil water retention curve (SWRC) and the soil hydraulic conductivity curve (SHCC) are essential functions for numerical physics-based models in soil science. In this regard, Hill and Sumner (1967) studied the influence of the variation in the soil bulk density on the soil water retention curve (SWRC) in artificially compacted soils and found that higher-density soils tend to exhibit a lower water holding capacity than lower-density soils due to reductions in the total pore space and pore connectivity. Smith et al. (2001) showed that compaction tends to flatten the typical S-shaped of the SWRC. Their analysis shows that for high matric potentials (from 0 to −10 kPa), compaction causes a reduction in water content and an increase in water content for low matric potentials (from −250 to −1,550 kPa). Their study shows a decrease in macropores and an increase in micropores could explain this hydraulic behavior. Above the SWRC inflection point are empty structural pores, and below are mainly empty textural pores (Alaoui et al., 2011).

In addition, compaction considerably influences flow and solute transport in soils. For instance, preferential flow increased for sieved, and reconditioned, and compacted sandy loam samples (Mooney and Nipattasuk, 2006). The rate of flow through a soil is directly proportional to the hydraulic conductivity of the soil. Alaoui et al. (2011) show that compaction causes a decrease in saturated soil hydraulic conductivity (Ks) in a context of reduced tillage of loamy soil with a low organic matter content. Specifically, the study found that as soil compaction increased, the saturated hydraulic conductivity decreased with a bulk density range of 1.3–1.5 g/cm^3 and a low organic matter content of 0.9%. However, Mossadeghi-Björklund et al. (2016) revealed an increased hydraulic conductivity near saturation for water contents below field capacity which they claim is a result of increased connectivity between small pores as a result of compaction. Other studies have shown that compaction causes a reduction in conductivity and pore connectivity (Hansson et al., 2018). These conflicting results imply that the quantification of the physical effects of soil compaction is complex.

The impact of soil compaction on water flow patterns in agricultural soils depends on prevailing conditions (soil erosion, soil acidification, Soil organic matter depletion etc.) (Zhang et al., 2006) but are still poorly understood (Mossadeghi-Björklund et al., 2019). In order to overcome this limitation, many experimental methods have been developed and tested over the years. A widely used experimental method is the simplified evaporation method (SEM) (Schnider, 1980) based on the method of Wind (1968). This method has many advantages over the traditionally used methods that include the pressure plate apparatus, the dew point method, and the sand box method (Schelle et al., 2013). It is a useful tool for quickly estimating SWRC of soil samples in the field or laboratory and is considerably simpler and faster to perform.

The HYPROP© automated device (Hydraulic Property Analyzer, Meter Group Inc., Pullman, WA, USA) is based on this method. It generates a high-resolution hydraulic dataset with excellent results compared to traditional approaches such as multistage flow (Schelle et al., 2010; Zhuang et al., 2017). This method is often combined with a WP4C potentiometer (Decagon Devices, Inc. Pullman, WA, USA) to accurately estimate the water content on the dry portion/range of the SWRC and interpret and model the soil water behavior. This modeling approach can be combined with a laboratory experiment to analyze changes in retention and unsaturated conductivity (Kuang et al., 2021). It also relates these hydrological characteristics to the physical properties of the soil (soil bulk density). It is the most practical method with a relatively high degree of confidence (Haghverdi et al., 2020) and can be used to collect experimental data, but collecting enough data to create the entire SWRC and SHCC can be difficult, so the numerical modeling is necessary.

Soil hydraulic models are mathematical representations of the relationships between the soil water content, soil water potential, and hydraulic conductivity. These models can be used to fit experimentally obtained data to predict water movement in soil and to help better understand the effects of soil properties on soil hydrology. Among the most popular soil water behavior models are the van Genuchten (1980) model and the Peters et al. (2015) model, accounting for the effect of film and flow in very dry soils. These models may not adequately describe the behavior of soils under all conditions, so it is crucial to investigate the performance of these models before performing any hydrological simulation. The van Genuchten and Peters models are being discussed as a comparison and validation of the results obtained from the HYPROP with a WP4C potentiometer. In this perspective, our study hypothesizes that soil hydrodynamic parameters, that are mainly represented by the SWRC and SHCC, differ as a function of

compaction levels. Then, we simulated soil compaction scenarios using HYDRUS-1D software with the dual porosity model in order to calculate the irrigation amount for different compaction levels which is beneficial for future agricultural practices. The general objective is therefore to investigate the effect of compaction on the hydrodynamic properties of cultivated soils using the HYPROP evaporation measurement device with an extended measurement range. The specific objectives are to:

1. Evaluate and compare the performance of retention and unsaturated conductivity models for different levels of compaction.
2. Estimate the variation in hydrodynamic parameters for compacted soils, including determining the effects of increasing bulk density on the SWRC as well as the SHCC.
3. Test compaction scenarios in the context of precision irrigation using HYDRUS-1D.

The paper is structured as follows: Section 2 presents the materials and methods applied to conduct the experiments; Section 3 discusses the results obtained for each specific objective including a case study that simulates precision irrigation scenarios for the potato crop; Section 4 highlights some of the obtained results, which are compared with those in the literature; and Section 5 summarizes and concludes the paper.

3. Materials and methods

3.1. Soil sample characteristics

The study was conducted on loamy sand soils obtained from a potato field (Goldrush species) in Dolbeau-Mistassini (48° 51′ 31″ N, 72° 11′ 50″ W) in Québec, Canada. The collected soils were homogenized then air-dried and passed through a 2-mm sieve. The soil's particles size properties (sand-silt-clay) were determined using the laser diffraction method (Mastersizer 2000 with liquid sampling hydro 2000, MALVERN instruments Ltd., WOR, UK) and according to the USDA classification. Soil organic matter content was determined by the loss on ignition method (CEAEQ, 2003) and the soil water pH was measured after the samples were air dried using an Orion 4-star meter benchtop pH/ISE meter (Thermo Fisher Scientific Inc, USA). The soil contains 82.32% sand, 17.67% silt, 0% clay, 5.04% organic matter and a pH of 4.76.

3.2. Measurement procedure

Five levels of soil compaction (C0: 0%, C30: 30%, C40: 40%, C50: 50%, and C70: 70%) were developed by artificially compacting the soil for a bulk density of 1.0, 1.3, 1.4, 1.5, 1.7 g/cm^3, respectively, in sample rings of 250 ml (Ø 80 mm, 50 mm height). The sample is compacted by dropping a standard hammer from a specified height onto the sample in the container. The compaction process is repeated several times until the desired level of compaction is achieved. The experiments were carried out in four replicates for each soil compaction level. The saturated hydraulic conductivity Ks was determined using the constant head method (Reynolds and Elrick, 2002). The pF (pressure head) value, together with the WC (water content), is used to describe the soil moisture level. The WC for the pF/WC curve and the unsaturated hydraulic conductivity were measured for the different compaction levels using the hydraulic proper analyzer (HYPROP, Meter Group, Pullman, Washington) combined with WP4C (PotentioMeter, Meter Group, Pullman, Washington) according to the instructions from the operation manual. The export, evaluation, and fitting of the measuring data were performed using HYPROP-VIEW and HYPROP-Fit software (Pertassek et al., 2015).

3.3. Models

We have simulated the 16 soil hydraulic models included in the HYPROP-Fit software grouped into four categories: original unimodal, PDI variants, bimodal variants, and bimodal-PDI variants. These models are used to simulate and predict water movement in the soil and to help understand the effects of soil properties on soil hydrology. The first category comprises the Brooks and Corey (1964) model, the Fredlund and Xing (1994) model, the Kosugi (1996) model, the van Genuchten (1980) constrained model (VG model), and the unconstrained model (VGm model). These models are also included in the other categories, except for the Brooks and Corey model. The bimodal variants did not contain the Fredlung and Xung model either.

In general, the bimodal model of the soil hydraulic models assumes that the soil consists of two distinct categories of pores and the PDI (pore-size distribution index) model considers the distribution of pore sizes and their associated hydraulic conductivities. The VG model is the most widely used for SWRCs and several researchers have attempted to improve the performance of the van Genuchten-Mualem (VGm) model (Kuang et al., 2021), including modifications to the model parameters and incorporating additional soil properties. Some studies have reported improved accuracy in predicting soil water content and hydraulic conductivity using these modified VGm models. However, the success of these attempts may depend on the specific soil properties and conditions being modeled.

3.4. Water retention curve fitting

This section introduces the VGm-b-PDI model, which is a variation of the bimodal unconstrained van Genuchten model and uses the Peters-Durner-Iden parameterization (Peters, 2013). The saturation function of water adsorption Sad is defined by the following expression:

$$Sad = 1 + \frac{1}{x_a - x_0}\left\{x - x_a + b\,\ln\left[1 - exp\left(\frac{x_a - x}{b}\right)\right]\right\} \quad (1)$$

$$b = 0.1 + \frac{0.2}{n^2}\left\{x - x_a + b\,\ln\left[1 - exp\left[-\left(\frac{\theta r}{\theta s - \theta r}\right)^2\right]\right]\right\} \quad (2)$$

x_a and x_0: are pF values at suctions at ha (ha: the suction at the air entry for the adsorptive retention) and h_0 [h_0: the soil tension

at zero water content ($10^{6.8}$ cm, corresponding to the oven dry conditions at 105°C, respectively; b: is the shape parameter and it is calculated using the equation below; n: the SWRC shape parameter; θ_r and θ_s: are the residual and saturated water contents of the soil, respectively (cm^3/cm^3)].

The scaled weighted sum of the two unimodal subfonctions and can be expressed as follows:

$$S\theta\left(h\right) = (\theta s - \theta r)\frac{\left(\sum_{i=1}^{2} w_i\,\Gamma\left(h\right)_i\right) - \Gamma_0}{1 - \Gamma_0} + \theta r\ Sad \tag{3}$$

$$\Gamma\left(h\right) = \left[\frac{1}{1 + (\alpha h)\ n\ )}\right]^m \ For\ the\ VG_m\ model \tag{4}$$

$\Gamma\left(h\right)$: is the basic saturation function and is calculated using the previous equation; Γ_0: is the basic function at h = h0; wi: weighting factor for the subfunction and $0 < w_i < 1$; m: shape parameter; h: suction; α: curve shape parameter

$$\sum w_i = 1. \tag{5}$$

3.5. Unsaturated hydraulic curve fitting

The soil unsaturated hydraulic properties were described using the PDI model of Peters (2013) that considers the film and the corner flow properties in arid soils and it is the sum of the capillary and the film conductivities (Rudiyanto et al., 2020). The equations are not shown here due to their mathematical complexity, but the reader can consult Peters et al. (2015) for more information.

3.6. Choice of performance criteria

The accuracy of the model predictions of the soil water content and unsaturated conductivity was evaluated based on four statistical parameters namely:

The mean bias error (MBE):

$$MBE = \frac{1}{n}\sum_{i=1}^{n}(E_i - M_i) \tag{6}$$

The mean absolute error (MAE):

$$MAE = \frac{1}{n}\sum_{i=1}^{n}|E_i - M_i| \tag{7}$$

The root mean square error (RMSE):

$$RMSE = \sqrt{\frac{1}{n}\sum_{i=1}^{n}(E_i - M_i)^2} \tag{8}$$

The correlation coefficient (r):

$$r = \frac{\sum_{i=1}^{n}\left(E_i - \overline{E}\right)\left(M_i - \overline{M}\right)}{\sqrt{\sum_{i=1}^{n}\left(E_i - \overline{E}\right)^2\ \sum_{i=1}^{n}\left(M_i - \overline{M}\right)^2}} \tag{9}$$

Where E and M are, respectively, the fitted and the measured values of SWRC and conductivity data, $\overline{E}$ et $\overline{M}$ are the adjusted and measured mean values of SWRC and conductivity data and n the number of data points.

The lower the value of MAE, the higher the accuracy of the model. The RMSE measures the amount of error between two data sets and the lower RMSE values indicate a better model fit. The MBE indicates the average bias of the prediction and a value of zero indicates perfect agreement between the observed and predicted values. However, the closer the value of r is to one, the better the fit of the model between simulated and observed data.

3.7. Statistical analysis

The statistical analyses have been performed using R v4.1.2 statistical analysis software (R Core Team, 2019). The normality of the data was recognized using the Shapiro-Wilk test and the homogeneity of variance was validated using the Levene's Car Packet Test (Fox and Weisberg, 2020). Differences are considered significant when p values are less than 0.05 (LSD test, $p < 0.05$) including ANOVA test followed by Tukey's test using the Agricolae package (Mendiburu, 2019).

3.8. Calculation of the plant available water

The readily available water (RAW), commonly measured as the difference in the volumetric water content between the soil potential at −33 and −1,500 kPa, is defined by:

$$RAW = MAD \times (\theta_{-33} - \theta_{-1500}) * D_r(mm) \tag{10}$$

It is the amount of available water before irrigation is required (IA, 2005).

Where:

- MAD is the maximum allowable depletion or deficit (%), and typical values for MAD are given by Doorenbos et al. (1979) in table format for nine rates of maximum evapotranspiration and four crop groups according to stress sensitivity.

Soil matric potentials (SMP) of −33 and −1,500 kPa are, respectively, field capacity (FC) and permanent wilting point (PWP), which are frequently used as indicators of soil water content (Kirkham, 2005).

In our case study, we defined the water availability (WA) as the difference in the volumetric water content between the potato soil matric potential at −15 and −30 kPa. These thresholds were determined in a previous study of Matteau et al. (2021). It is estimated using the equation below:

$$WA = (\theta_{-15} - \theta_{-30}) * D_r(mm) \tag{11}$$

Where: WA is the amount of water available to plants (mm); θ_{-15} is the volumetric water content at −15 kPa (cm^3/cm^3); θ_{-30} is the volumetric water content at −30 kPa (cm^3/cm^3); Dr is the depth of the root zone or depth of a layer of soil within the root

TABLE 1 Soil physical properties.

Soil properties	Min	Max	SD [g]	Mean
BD (g/cm^3)[a]	1	1.7	0.24	1.38
pF (–)[b]	−0.147	6.28	0.70	2.25
θ (cm^3/cm^3)[c]	0.00	0.5185	0.03	0.32
θ_s (cm^3/cm^3)	0.37	0.63	0.09	0.49
Initial water content (%)	41.2	51.88	2.80	45.52
Dry weight (g)[d]	241.4	414	56.61	335.55
Density (g/cm^3)[e]	0.97	1.66	0.23	1.35
Porosity (–)[f]	0.37	0.63	0.09	0.49

[a]BD, bulk density of soil; [b]pF, log (h) where h is soil tension (cm water column); [c]θ, water content of soil measured by HYPROP and WP4C instrument (s, saturated water content); [d]Dry weight, after drying at 105°C for 24 h; [e]Density, soil bulk density; [f]Porosity, calculated from bulk density, assuming a solid density of 2.65 g/cm^3; [g]SD, standard deviation; "(–)" means unitless.

TABLE 2 Overall performance of the SWRC models.

Model	MBE	MAE	*r*
BC	0.0003	0.0379	0.909
FX	0.0002	0.0373	0.913
FX-PDI	0.0051	0.0368	0.913
FX-b-PDI	0.0026	0.0367	0.914
K	0.0004	0.0379	0.911
K-PDI	0.0007	0.0373	0.913
K-b	0.0003	0.0371	0.914
K-b-PDI	0.0032	0.0366	0.913
VG	0.0002	0.0379	0.912
VG-PDI	0.0001	0.0371	0.913
VG-b	0.0003	0.0373	0.913
VG-b-PDI	0.0000	0.0369	0.914
VGm	0.0003	0.0377	0.912
VGm-PDI	0.0006	0.0371	0.913
VGm-b	0.0004	0.0372	0.913
VGm-b-PDI	0.0003	0.0361	0.914

BC, Brooks and Corey; FX, Fredlund and Xing; K, Kosugi; VG and VGm, van Genuchten unimodal constrained and unconstrained soil water retention models; PDI and b denote the Peters-Durner-Iden and bimodal variants of the models, respectively; MAE, mean absolute error (cm^3/cm^3); MBE, mean biased error (cm^3/cm^3); *r*, correlation coefficient.

zone (mm) and can be found in a table compiled by Doorenbos and Pruitt (1977) and Maas and Hoffman (1977).

4. Results

4.1. Soil physical characteristics

The results of the measurements from the replicates for each compaction level were averaged to determine the water retention and conductivity. The logarithmic transformation of water tension (pF values) ranged from −0.147 to 6.28. The measured saturated water content ranged from 0.37 to 0.63 and was calibrated with the porosity values, with an average θ_s value of 0.49 cm^3/cm^3. The initial water content ranged from 41.2 to 51.88%. Table 1 provides an overview of some of the physical properties of the soil (average values of the replications).

TABLE 3 RMSE of SWRC for different compaction levels.

Model	RMSE(θ)				
	C0	C30	C40	C50	C70
VGm-b-PDI	0.0152	0.0139	0.0091	0.0092	0.0122
FX-b-PDI	0.0152	0.0140	0.0094	0.0093	0.0122
K-b	0.0158	0.0144	0.0101	0.0094	0.0122
VGm-b	0.0153	0.0140	0.0095	0.0092	0.0123
K-b-PDI	0.0152	0.0139	0.0093	0.0101	0.0123
VG-b-PDI	0.0153	0.0140	0.0094	0.0093	0.0124
VG-b	0.0153	0.0141	0.0097	0.0093	0.0124
VGm-PDI	0.0170	0.0146	0.0096	0.0097	0.0129
VG-PDI	0.0172	0.0146	0.0098	0.0097	0.0129
FX-PDI	0.0176	0.0150	0.0097	0.0098	0.0131
FX	0.0181	0.0148	0.0098	0.0098	0.0132
K-PDI	0.0177	0.0150	0.0103	0.0101	0.0133
VGm	0.0194	0.0169	0.0117	0.0112	0.0144
VG	0.0198	0.0180	0.0139	0.0123	0.0149
K	0.0209	0.0195	0.0159	0.0139	0.0159
BC	0.0220	0.0201	0.0140	0.0144	0.0175

RMSE, root mean square error (cm^3/cm^3).

4.2. Assessment of models overall performance

For the SWRC, results showed that the VGm-b-PDI model has the best performance with an RMSE of 0.0469 cm^3/cm^3 (MAE of 0.0361 cm^3/cm^3) followed by the K-b model with an RMSE of 0.047 cm^3/cm^3 (MAE of 0.0371 cm^3/cm^3). Model BC showed the lowest accuracy with an RMSE of 0.0483 cm^3/cm^3 (MAE 0.0379 of cm^3/cm^3). The r values ranged from 0.909 to 0.914 with the lowest r observed for model BC and comparable values for the other models. We summarized the performance of the extended water-retention function and presented the overall result with the statistical parameters in Table 2. Table 3 show the model error distributions as RMSE for θ for the different compaction levels.

We evaluated the performance of the models for the soil hydraulic conductivity curve (SHCC) by calculating the RMSE values of HYPROP-Fit, which represent the difference between the measured and estimated log10(K) data. The RMSE values for the different compaction levels are displayed in Table 4, and they are all close to the assumed measurement errors of n for the logarithmic conductivity data. The hydraulic model did not reveal

TABLE 4 RMSE of log10(K) for different compaction levels.

Model	RMSE (log10K)				
	C0	C30	C40	C50	C70
VGm-PDI	0.1130	0.0279	0.0247	0.0653	0.4003
VG-b-PDI	0.1153	0.0369	0.0302	0.0724	0.4269
VG-PDI	0.1200	0.1642	0.0288	0.0710	0.4219
FX-b-PDI	0.1249	0.0280	0.0283	0.0671	0.4092
K-b-PDI	0.1274	0.0383	0.0321	0.0693	0.4180
VGm-b-PDI	0.1382	0.0295	0.0298	0.0997	0.4613
FX-PDI	0.1397	0.0351	0.0267	0.0654	0.4077
K-PDI	0.1423	0.0569	0.0407	0.0681	0.4124
VGm-b	0.1556	0.0341	0.0494	0.0807	0.4444
VG	0.1646	0.1027	0.0978	0.0703	0.4190
FX	0.1683	0.0572	0.0510	0.0654	0.4021
BC	0.1810	0.0890	0.0875	0.0734	0.4371
VG-b	0.1816	0.0417	0.0401	0.0723	0.4255
VGm	0.1835	0.0899	0.0877	0.0725	0.4303
K	0.1928	0.1452	0.1246	0.0677	0.4119
K-b	0.1979	0.0874	0.0547	0.0689	0.4131

any bimodal behavior, and the PDI model was found to be well-suited to express it. Among the models tested, VGm-PDI showed the best performance for the SHCC.

4.3. Soil hydraulic characteristics

The SWRC and the SHCC that have been fitted with the van Genuchten models are detailed in the next section.

4.3.1. Soil water retention

The soil water retention data was fitted using the van Genuchten's unconstrained bimodal PDI model (VGm b-PDI). The figure below (Figure 1) shows the water retention curves measured with the extended range of evaporation measurements for each compaction level.

The relationship between water content and pF changed more drastically over small changes in pF values. The water content decreases linearly in the suction range and varied with the compaction levels in both humid and dry range. In the humid range, which is generally defined as pF values between 1 and 3, the volumetric water content tends to be higher for more compacted soils, and lower for less compacted soils. In the dry range, which is generally defined as pF values between 3 and 4.2, the relationship between compaction level, pF, and water content is more consistent. As the soil becomes more compacted in the dry range, the available soil water decreases and the pF value increases. This means that for a given compaction level, the soil will hold less water at higher pF values.

4.3.2. Saturated hydraulic conductivity

The saturated hydraulic conductivity Ks (cm/day) for the five compaction levels is presented in Figure 2. Results show that Ks decreased when soil bulk density increased, and the lowest Ks value is due to the existence of a solid medium and least connected pores as soil compaction level increases. We also assumed that the remaining conductivity parameter Ks values might need a correction in the HYPROP-Fit because the instrument provides unreliable K(pF) data near saturation and overestimates the saturated conductivity values according to the HYPROP-Fit manual.

4.3.3. PDI hydraulic conductivity model

The PDI-variant of the unconstrained van Genuchten model (VGm PDI) model is the most accurate for unsaturated conductivity and was used to simulate the SHCC after forcing the Ks values into the HYPROP-Fit software. Figure 3 shows the observed hydraulic conductivity data as a function of pressure head. The SHCC decreases with increasing matric suction due to dry pores blocking water flow (Zhai and Rahardjo, 2015). Furthermore, the conductivity estimates for the C50 and C70 groups are aligned because the soil structure becomes more homogeneous, which means that the distribution of pores is more uniform, resulting in a consistent hydraulic conductivity.

4.3.4. Tortuosity, air content and diffusivity calculations

The tortuosity designed by ξ(−) is a connectivity parameter for gas transport, which is considered as a fitting parameter. The value of the gas tortuosity parameter cannot be directly measured, but it was calculated from Millington and Quirk (1961) and represented in the equation below:

$$\xi = \frac{\theta_a^{\frac{7}{3}}}{\theta_s^2} \tag{12}$$

Where: θ_s and θ_a are the saturated water and air contents of the soil, respectively (cm^3/cm^3): Tau: empirical parameter for the conductivity function, related to pore tortuosity and pore connectivity; omega: weight parameter for film flow contribution to the hydraulic conductivity.

Table 5 summarizes the different values of the calculated parameters. In this table we can notice that the total porosity Φ and the air content decrease with increasing bulk density for potentials 6, 18, 33, 1,500, 6–1,500, and 33–1,500 kPa. Gas tortuosity values based on the formula of Millington and Quirk (1961) are proportional to air content θ_a and inversely proportional to saturated water content θ_s and decrease when bulk density values increase. Thus, according to Penman (1940a,b), gas tortuosity values also reduced, and ξ (θ) values increased with higher compaction levels for different values of matric potentials.

The average value of air diffusivity Da is 2.46 E-05, decreasing with increasing soil bulk density for different values of matric potentials.

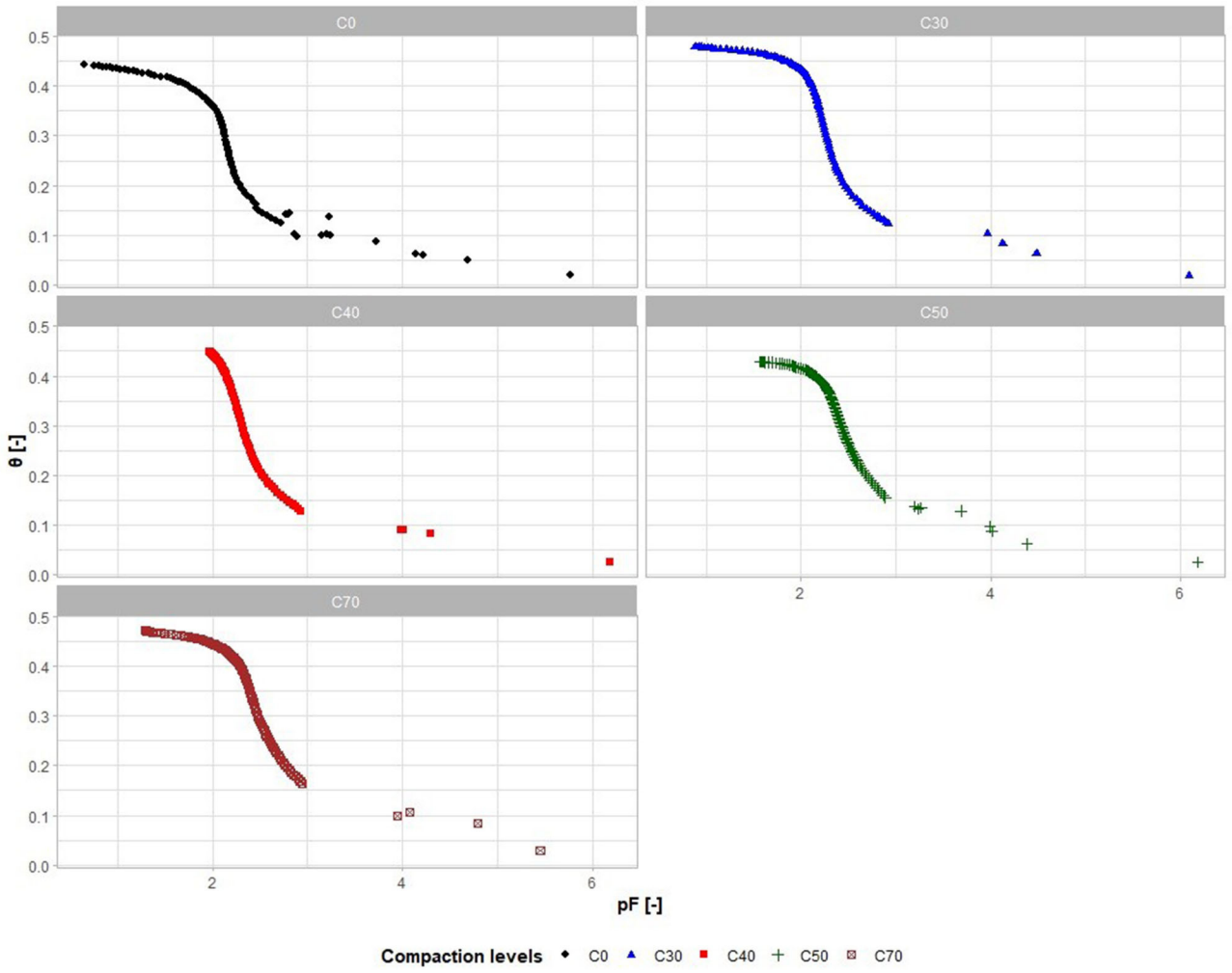

FIGURE 1
Measured soil water retention curves as function of matric potential at different compaction levels (C0, 0%; C30, 30%; C40, 40%; C50, 50%; and C70, 70%).

4.4. Influence of compaction levels on models parameters

The statistical results show that the means of the model parameters (VGm b-PDI; VGm PDI) of all compaction levels are considered equal. The analysis indicated that these parameters varied significantly with the effect of compaction levels. The estimated SWRC parameters using the VGm b-PDI model are listed in Table 6. A Principal Component Analysis (PCA) was performed across the compaction level to identify the most strongly related parameters of the retention and conductivity functions. The parameters n1, n2, m1, θ_r, and θ_s are those that have more contribution to the SWRC model.

The curve-shape parameters n1 and n2 are related to the pore size distribution in the matric domain (Meurer et al., 2020). The mean values of the parameter n1 (shape parameter for the width of the bimodal retention curve) vary from 1.01 to 11.407. For n2 (shape parameter for the bimodal retention curve), the mean values vary from 5.0075 to 15. The differences in the parameter n1 and n2 are significant and values of the parameter m1 are also more variable and range from 0.128 to 1. The residual water content θ_r refers to the soil matric that decreases rapidly with insignificant changes in water content and it varies among different compaction levels and ranges from 0.11 to 0.13 cm^3/cm^3. The saturated water content θ_s varies from 0.45 to 0.49 cm^3/cm^3.

The PCA indicated that the unsaturated conductivity parameters including Ks, tau and omega have significant contributions too. As the compaction level increased from C0 to C70, the tau values increased from 0.6 to 1.3 and the omega values ranged from 7.83E-05 to 1.02E-03. Mean values, standard deviations and standard errors are provided for each measurement in Table 7.

4.5. Effect of soil compaction on plant available water

Based on the previous work of Matteau et al. (2021), the matric potential levels −15, −18, and −30 kPa were selected corresponding to the lower, optimum, and upper limits,

respectively, for highest potato (Goldrush species) marketable yield. The variation of the water depth for the selected matric potential levels are shown in Figure 4. The results show a general increase in water content values with increasing compaction level from C0 to C70.

The comparison between the readily available water RAW at −33 and at −1,500 kPa and the Water availability (WA) in the optimal matric potential range for potatoes at −15 and at −30 kPa with the compaction level is shown in Figure 5. The RAW increases considerably with increasing compaction level and in contrast the WA increases to C40 and then drops to zero.

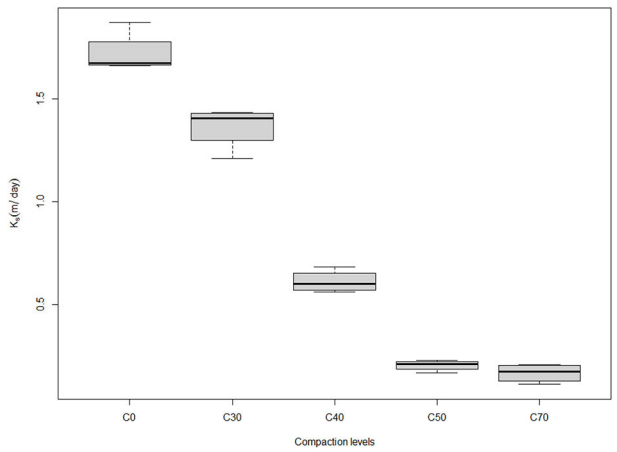

FIGURE 2
Measured saturated hydraulic conductivity at different compaction levels by the constant head test.

4.5.1. Calculation of the water-filled pore space

The water-filled pore space (WFPS) is determined by water content and total porosity (Farquharson and Baldock, 2008) and the calculation was realized with the following equation:

$$WFPS\,(\%) = \frac{Volumetric\ water\ content}{Soil\ porosity} * 100 \qquad (13)$$

For further evaluation of the relationship between compaction and WFPS, calculations were performed for the 3 SMP −15, −18, and −30 kPa. Figure 6 depicts the relationship between the compaction level and the WFPS performed at different soil matric potentials. Results show that increasing the soil compaction level from C0 to C70 increased the WFPS by 58.2, 66.03, and 72.29% for the −15, −18, and −30 kPa matric potentials, respectively, and these results agree with the findings of Balaine et al. (2016).

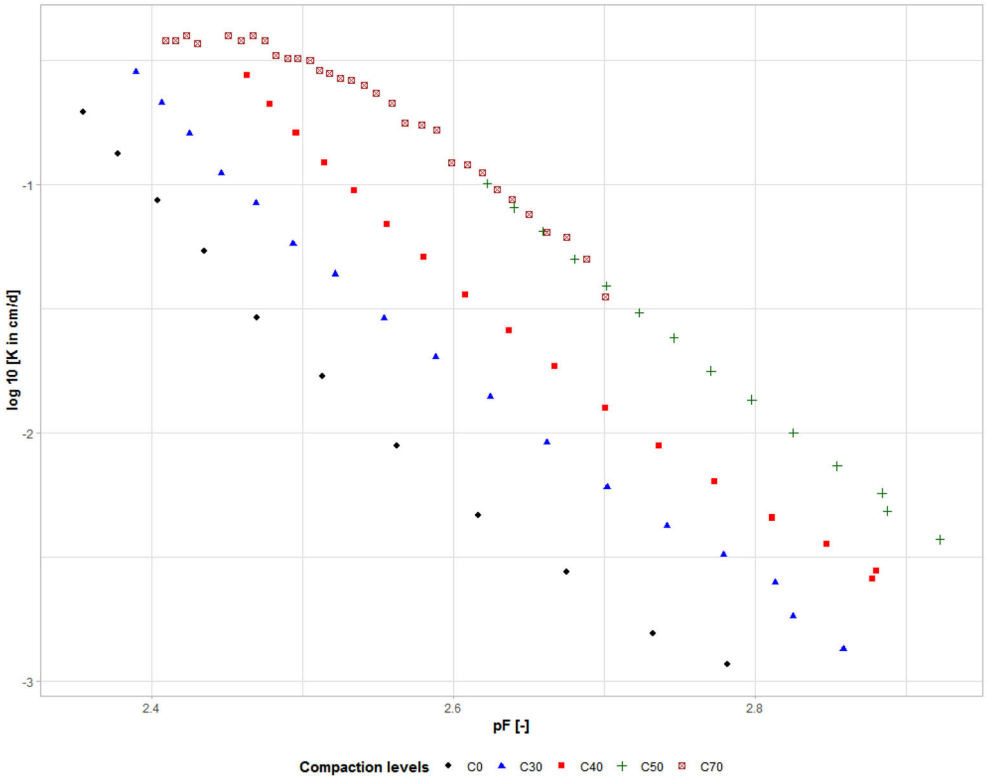

FIGURE 3
The measured unsaturated hydraulic conductivity as function of the matric potential at different compaction levels (C0, 0%; C30, 30%; C40, 40%; C50, 50%; and C70, 70%).

TABLE 5 Total soil porosity Φ, volumetric soil air content (θ_a), air diffusivity and vapor diffusivity.

Variable	Matric potential	Compaction levels				
		C0	C30	C40	C50	C70
Total soil porosity Φ, cm^3/cm^3	All kPa levels	0.63	0.52	0.4825	0.4425	0.3775
tau (–)	All kPa levels	0.59375	1.16225	0.813	0.83175	1.30125
Omega (–)	All kPa levels	7.83E-05	1.72E-04	5.11E-04	1.39E-03	1.02E-03
Soil volumetric air content (%vol)	6 kPa	5.415	2.483	1.615	0.775	3.325
	18 kPa	23.965	17.018	14.003	10.045	7.405
	33 kPa	30.643	29.345	27.34	21.608	19.25
	1.500 kPa	38.635	40.1925	40.0425	39.63	40.0525
	6–1,500 kPa	11.753	10.38	9.82	8.663	12.383
	33–1,500 kPa	36.98	37.378	35.548	26.055	28.5
Gas tortuosity (–) (Millington and Quirk, 1961)	6 kPa	0.027	0.005	0.002	0	0.014
	18 kPa	0.819	0.41	0.208	0.123	0.055
	33 kPa	1.454	1.148	0.968	0.576	0.417
	1,500 kPa	2.495	2.391	2.354	2.314	2.265
	6–1,500 kPa	0.161	0.102	0.089	0.08	0.148
	33–1,500 kPa	2.258	2.352	1.784	0.918	1.023
Gas tortuosity (–) (Penman, 1940a,b)	All kPa levels	0.416	0.343	0.318	0.292	0.249
Liquid tortuosity (–) (Millington and Quirk, 1961)	6 kPa	1.199	0.277	0.318	0.313	0.531
	18 kPa	0.014	0.076	0.122	0.2	0.382
	33 kPa	0.004	0.014	0.023	0.06	0.126
	1,500 kPa	0.0003	0.0008	0.0011	0.0013	0.0024
	6–1,500 kPa	0.0654	0.1477	0.1652	0.1539	0.2585
	33–1,500 kPa	0.0006	0.0023	0.0045	0.0167	0.0382
Vapor diffusivity D ($m^2\ s^{-1}$)	All kPa levels	2.48E-05	2.49E-05	2.44E-05	2.45E-05	2.46E-05
	6 kPa	3.72E-06	4.51E-07	1.43E-07	1.28E-08	2.73E-06
	18 kPa	4.88E-04	1.97E-04	7.56E-05	5.75E-05	1.55E-05
	33 kPa	1.11E-03	8.49E-04	6.54E-04	3.67E-04	2.16E-04
	1,500 kPa	2.40E-03	2.40E-03	2.31E-03	2.32E-03	2.26E-03
	6–1,500 kPa	4.90E-05	2.70E-05	2.15E-05	1.86E-05	4.86E-05
	33–1,500 kPa	2.28E-06	2.22E-03	1.55E-03	5.87E-04	1.50E-06

4.5.2. Estimation of field capacity

Assouline and Or (2014) revised the concept of field capacity by estimating effective soil saturation using Lehmann et al. (2008). We used this approach to calculate the water content at field capacity with the different levels of compaction (Figure 7). Using the Assouline and Or (2014) approach (Figure 7A), we can conclude that the SMP level of −33 kPa (Figure 7B) overestimates the water content at field capacity and is inappropriate not only for calculating irrigation volume for potatoes but also for calculating the RAW.

4.6. Case study: simulation of precision irrigation scenarios with HYDRUS-1D

To further study the effects of soil compaction on soil hydraulic properties, we simulated soil compaction scenarios using the HYDRUS-1D software (Šimunek et al., 2016). The dual porosity model (Gerke and van Genuchten, 1993) was used to account for the heterogeneity of the soil pore space. The estimated SWRC parameters using the bimodal-constrained model of van Genuchten (VGb) are listed in the Table 8.

10.3389/frwa.2023.1255495

TABLE 6 Mean parameters of the PDI variant of the bimodal van Genuchten-Mualem unconstrained water retention (VGm b-PDI) associated to different compaction levels.

Compaction levels	α1 (1/cm)	α2 (1/cm)	n1 (–)	n2 (–)	m1 (–)	m2 (–)	θ_r (cm^3/cm^3)	θ_s (cm^3/cm^3)
C0	0.4552 ± 0.089	0.0083 ± 0.000	1.0100 ± 0.000	10.6960 ± 3.4646	0.8315 ± 0.337	0.2955 ± 0.148	0.1318 ± 0.062	0.6300 ± 0.000
C30	0.1669 ± 0.226	0.1303 ± 0.246	5.7310 ± 6.670	9.0385 ± 4.235	0.7943 ± 0.411	0.3478 ± 0.060	0.1755 ± 0.033	0.5200 ± 0.000
C40	0.0124 ± 0.011	0.0050 ± 0.000	3.2975 ± 2.706	5.0075 ± 2.277	0.4453 ± 0.299	0.8935 ± 0.213	0.1528 ± 0.023	0.4825 ± 0.005
C50	0.0067 ± 0.005	0.0047 ± 0.000	2.4250 ± 2.208	7.1653 ± 2.799	0.7030 ± 0.442	0.3370 ± 0.175	0.1373 ± 0.026	0.4425 ± 0.005
C70	0.0021 ± 0.001	0.0038 ± 0.000	11.407 ± 7.186	15.0000 ± 0.000	0.0718 ± 0.035	0.7753 ± 0.449	0.1530 ± 0.034	0.3800 ± 0.010

TABLE 7 Statistical description of the unsaturated conductivity function parameters based on the VGm PDI model.

Variable	Minimum	Maximum	Average	SD
Ks	1.030	10,000.000	1,981.306	3,320.985
tau	−0.516	3.075	0.623	0.847
Omega	0.000	1,620,000.000	81,082.255	362,223.834

SD, standard deviation.

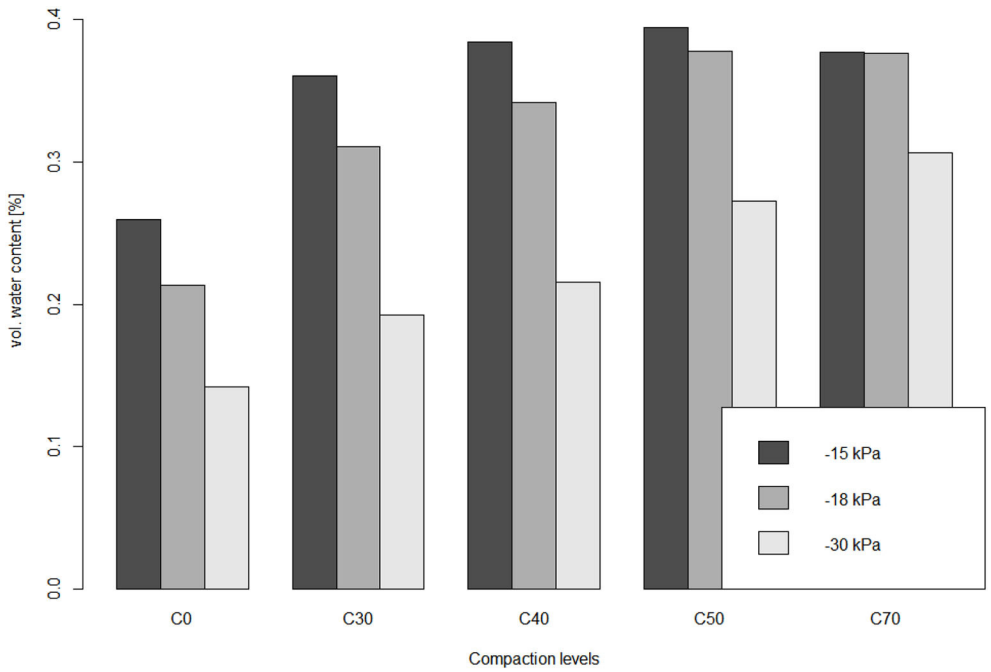

FIGURE 4
Water content for different soil water potentials levels (−15, −18, and −30 kPa).

For this study case, we used 153 days of 2018 of meteorological data from a potato field near Québec-City, Canada as input for the simulation. The simulation was performed for a depth of 100 cm with a time step of 1 day. Soil hydraulic properties were calculated using data from HYPROP with different compaction levels, namely C0, C30, C40, C50, and C70 corresponding to compaction percentage from the bulk density. The boundary conditions were set as top, atmospheric (Rainfall and evapotranspiration) in Figures 8A, B and at the bottom free drainage. We also add a trigged irrigation condition. Irrigation started based on the matric potential at the root zone (−180 cm), 20 mm was applied in 24 h when this condition was reached. Figure 9 shows the relationship between soil

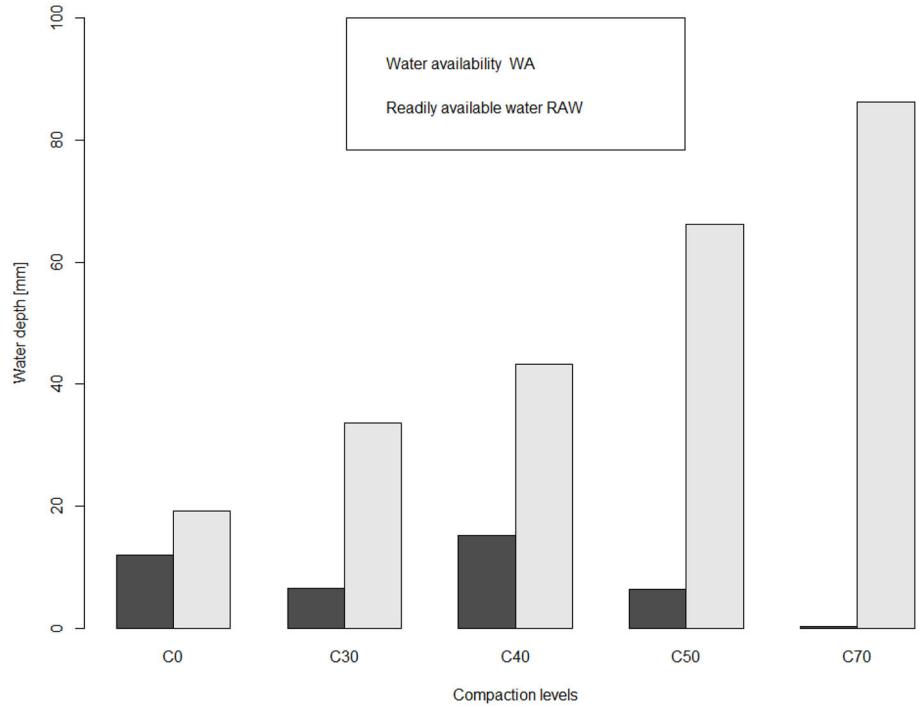

FIGURE 5
The water availability (WA) and the readily available water (RAW) with the compaction level.

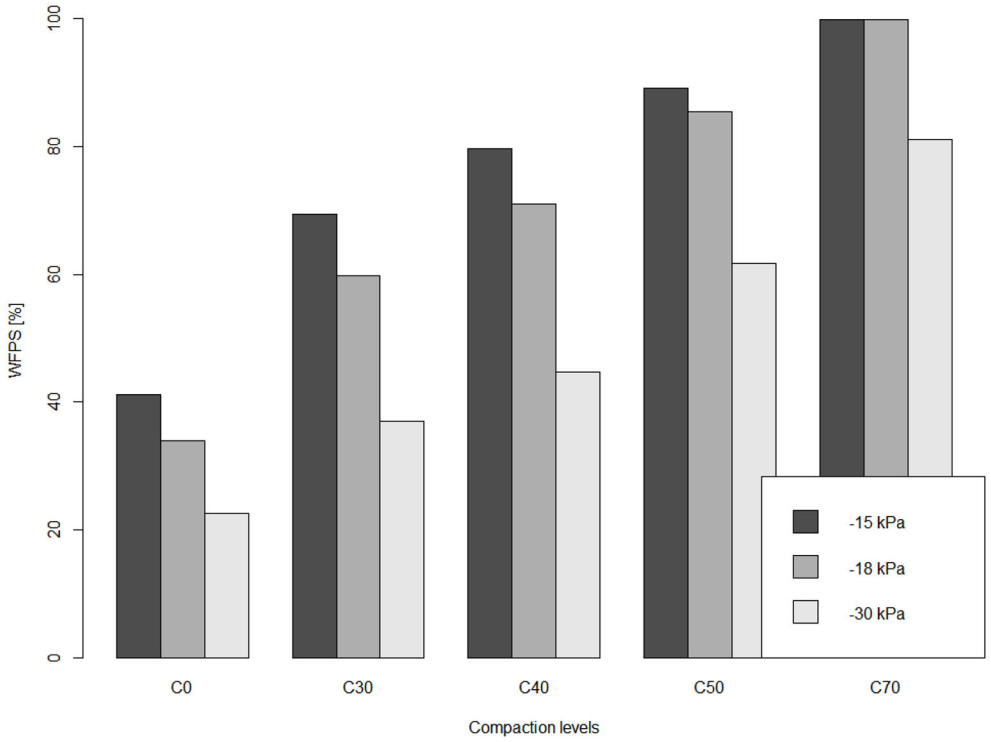

FIGURE 6
Water filled pore space (WFPS) (%) for different soil water potentials levels (at −15, −18, and −30 kPa).

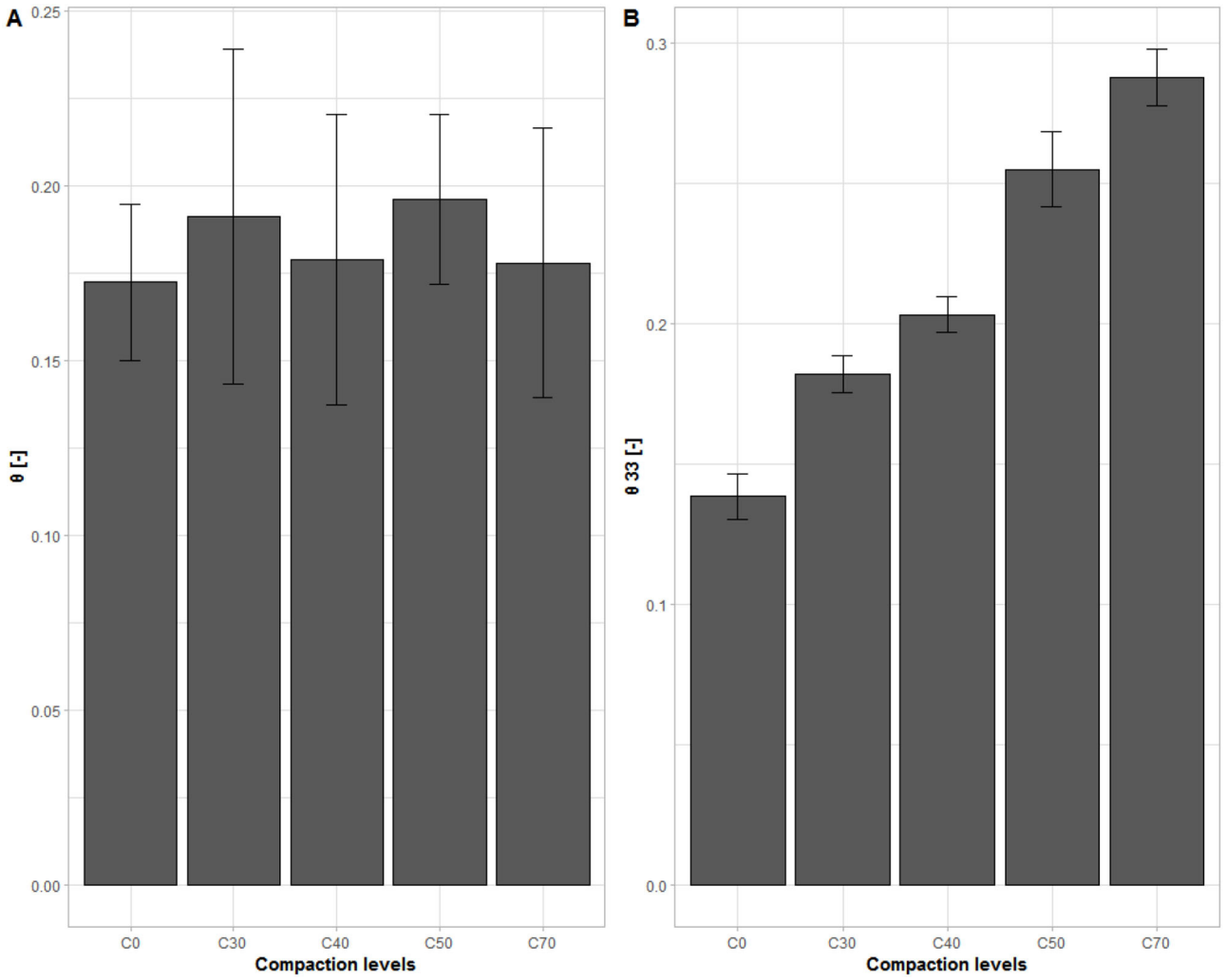

FIGURE 7
Water content at Field Capacity for different compaction levels. **(A)** Assouline and Or (2014) approach; **(B)** −33 kPa.

matric potential, soil moisture and soil hydraulic conductivity. The red lines on Figure 9 represent the irrigation limits, which indicate the beginning (−180 cm) and end (−250 cm) of the irrigation period. The SWRC data at the start time of irrigation shows that the water content expressed in cm^3/cm^3 for non-compacted soil (C0), low compaction (C30), and moderate compaction (C40) are, respectively, 0.175; 0.31, and 0.34. For a high level of compaction (C50) the water content decreased to 0.17 and then increases to 0.24 for an extremely high level (C70). It is observed that the unsaturated conductivity decreases as the soil matric potential increases. The unsaturated K values expressed in decimal logarithm (cm/day) increase from the C0 level to the C70 level but drops for C30. The shape of the SHCC can indicate the drainage properties of the soil. A steep curve indicates a soil with a high drainage rate, which represents low compacted soils, while a flat curve indicates a soil with a low drainage rate which are high (C50) and extremely compacted soils (C70).

Figure 10 shows the soil matric potential at the root zone (SMP), the volumetric water content for the 153 days of simulation, and the five compaction levels. We can see that the behavior is quite different for both the SMP and volumetric water content. During the beginning of the season, the soils have a water content of 40% and a matric potential value of −125 cm, then drop to −600 cm for the non-compacted soil (C0) with 11% water content and −450 cm for C70 with only 5%. The water flux took more time for C70 level when compared to less compacted soils within a period of 30 days. After that, we observe two irrigation peaks at days 80 and 90 to exceed 30% water content, and the SMP reaches −250 cm for the C50 level. The soil dries out differently depending on the degree of compaction and the volume of water increases with the increase of the compaction level but drops for the high and extremely high levels C50 and C70. Based on the calendar irrigation period, the optimum moisture range is between −200 and −400 cm and the lower and upper limits of water content are 0.15 and 0.25 cm^3/cm^3, respectively.

The idea was to see the effect of soil compaction on irrigation management. Figure 11 shows the irrigation amount for the five compaction levels. The volume of irrigation increases from C0

TABLE 8 Soil hydraulic bimodal VG parameters for HYDRUS modeling.

Compaction levels	α1 (1/cm)	α2 (1/cm)	n1 (–)	n2 (–)	θ_r (cm^3/cm^3)	θ_s (cm^3/cm^3)	w2 (–)
C0	0.031 ± 0.023	0.0069825 ± 0.0002	1.378 ± 0.134	7.1515 ± 1.490	0.0275 ± 0.0147	0.4555 ± 0.026	0.43325 ± 0.017
C30	0.017975 ± 0.005	0.00592 ± 0.0005	1.2115 ± 0.038	4.9655 ± 0.604	0.00375 ± 0.007	0.491 ± 0.023	0.5295 ± 0.034
C40	0.0068775 ± 0.005	0.005575 ± 0.0004	1.1932 ± 0.032	4.03475 ± 0.256	0 ± 0	0.4795 ± 0.016	0.60925 ± 0.028
C50	0.021505 ± 0.035	0.005285 ± 0.003	2.6932 ± 1.777	2.37075 ± 1.300	0.006 ± 0.0064	0.32965 ± 0.217	0.528 ± 0.072
C70	0.01776 ± 0.016	0.0048725 ± 0.003	2.1482 ± 1.910	3.14525 ± 1.418	0.00375 ± 0.007	0.48 ± 0.017	0.521 ± 0.083

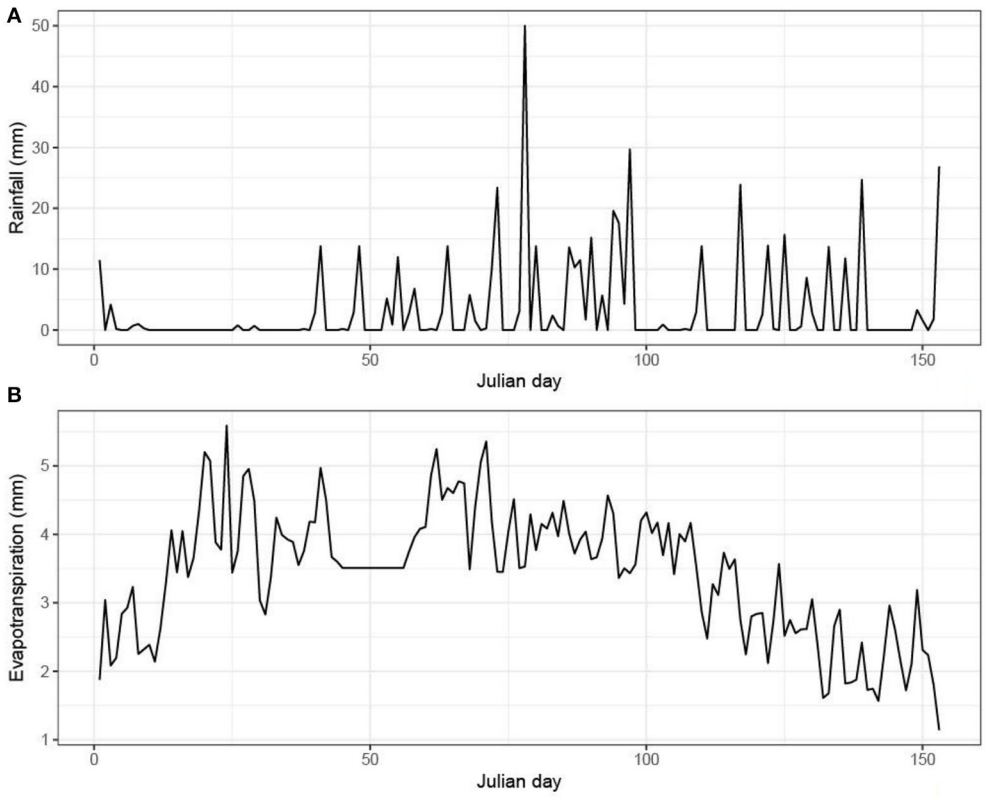

FIGURE 8
Simulation input parameters for the case of study of irrigation management. **(A)** Rainfall for growing season of 2018, including rainfall and irrigation; **(B)** The crop evapotranspiration for culture season of 2018.

to C30 and remains unchanged for C40. But the water content decreases at a high compaction level (C50) and increases slightly at an extremely high level (C70).

5. Discussion

In the present study, the HYPROP approach showed that the VGm b-PDI model presents satisfactory results for the soil water retention curves. According to METER Group (2023), the bimodal curve can be described as a "stair step" curve resulting from a pore size distribution that includes many small and large pores, but lacks medium-sized pores, which is referred to as a "gap-graded" pore size distribution. However, the unsaturated hydraulic conductivity curve performed well with the VGm PDI model and did not show bimodal behavior because it occurred outside the range of micropores identified with the WP4C dataset (Lipovetsky et al., 2020).

Another point of discussion is the increase of water content with compaction that causes an increase in water content leading to homogenization and, thus, a particle rearrangement. It is documented that the compacted soil layers have relic soil pores that are connected to structural pores, and they are responsible for the increase of the volumetric water content (Richard et al., 2001). Balaine et al. (2016) reported in their study that an increase in soil bulk density also affected the pore size distribution: soil macroporosity (pores with a diameter of >30 μm) decreased. Meanwhile, the mesoporosity (pores with a diameter of 30–0.2 μm)

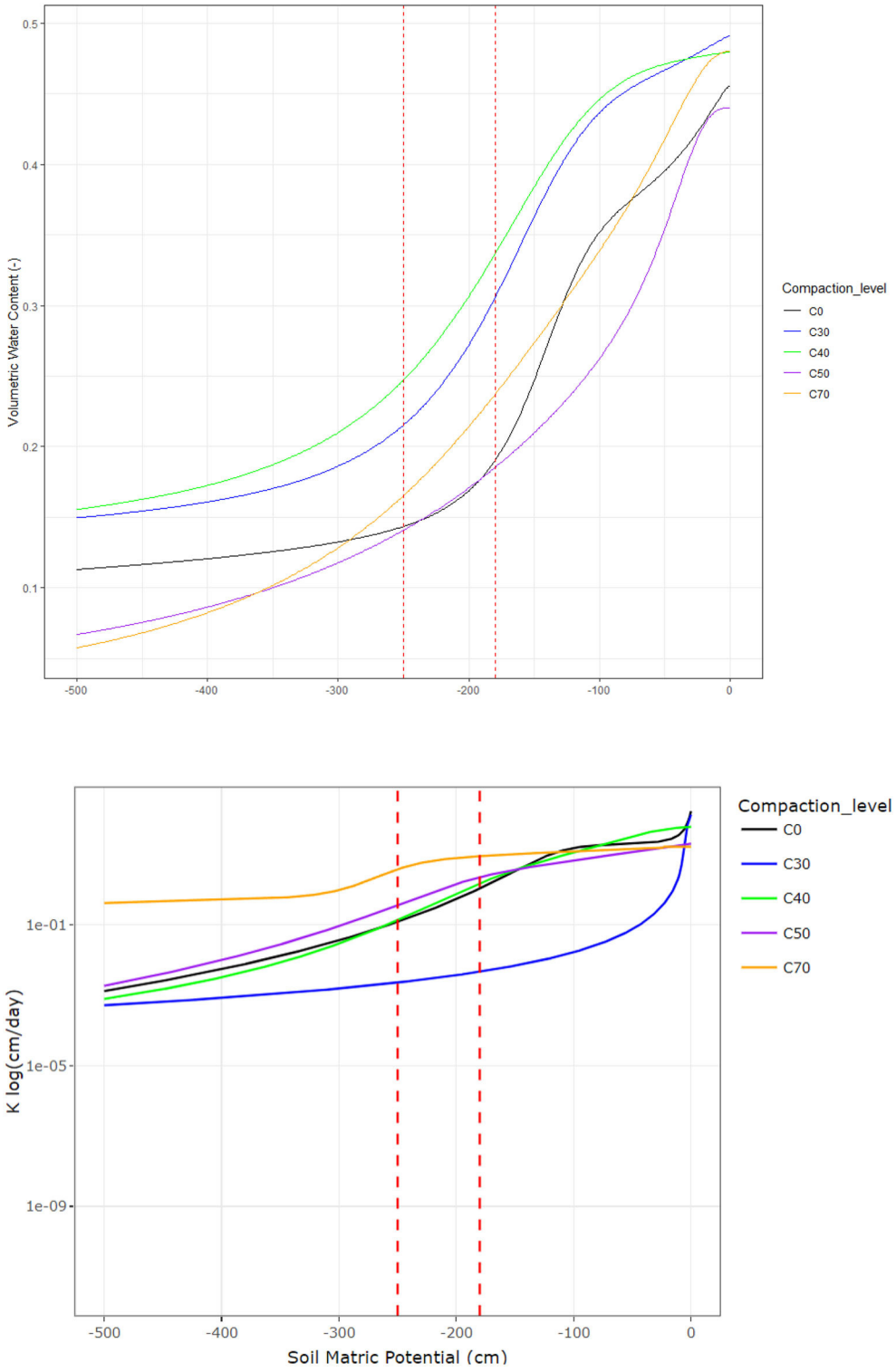

FIGURE 9
Retention and conductivity curves using the bimodal VG model for the five compaction levels using the HYPROP fitted parameters.

and microporosity (pores with a diameter of $<0.2\,\mu m$) increased. Parvin et al. (2017) indicate that the size of pore openings influences the drying process and that soils having an appropriate macropore amount but without good connectivity are not hydraulically efficient. Mossadeghi-Björklund et al. (2019) showed that the macropores ($\geq 0.3\,\mu m$) decreased from 10 cm (BD = 1.27 g/cm^3) to 30 cm (BD = 1.38 g/cm^3), but the large mesopores (0.3–0.006 μm), as well as the small mesopores (0.06–0.03 μm), increased.

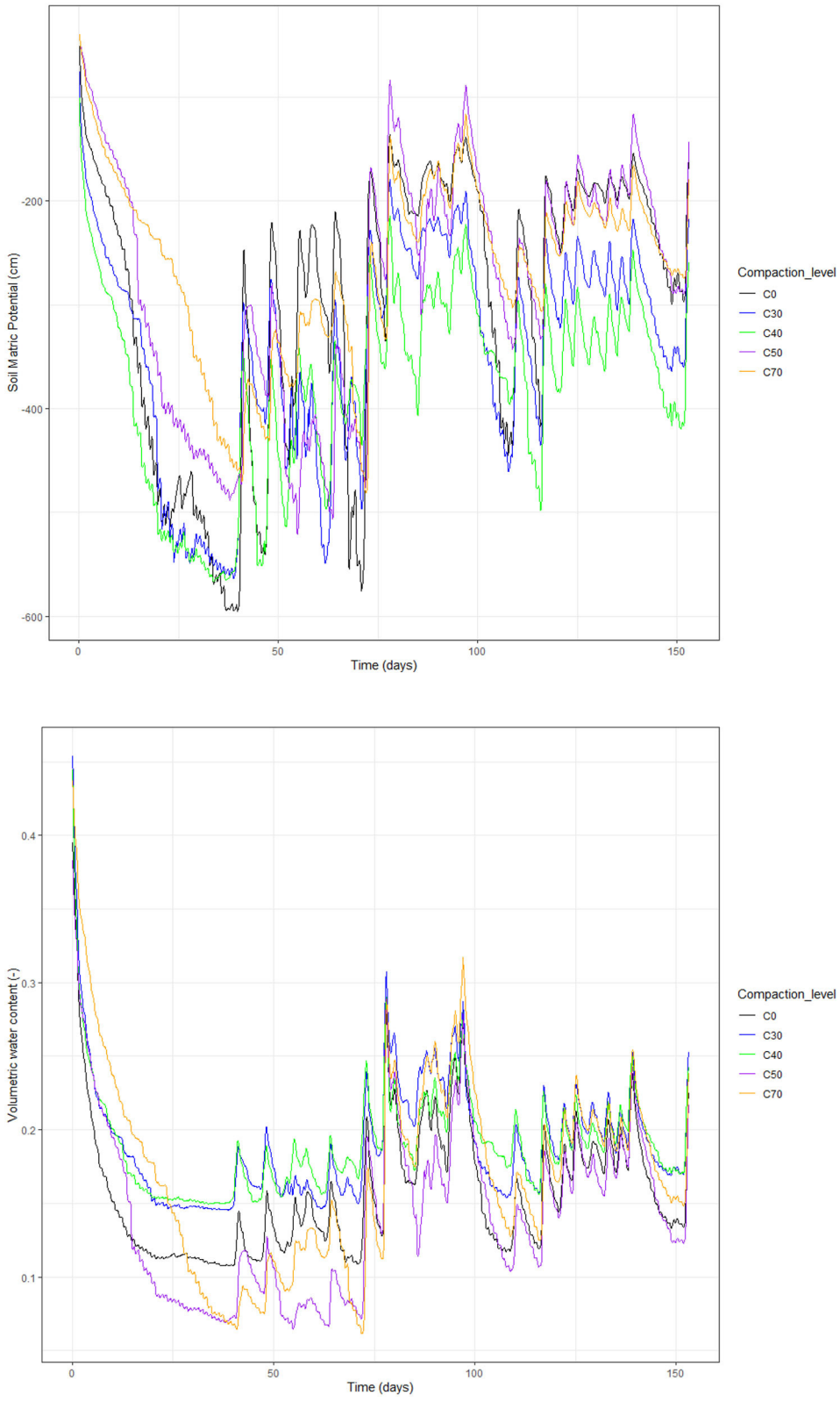

FIGURE 10
Soil matric potential (SMP) at 15 cm below the soil surface for the five compaction levels and the volumetric water content.

The RAW increase with increased soil compaction, depending on the initial soil water content and the level of compaction. However, when soil is compacted, in the same volume (as is the case here because the HYPROP cylinders all have the same volume), there are more soil particles, and therefore more water storage potential. Therefore, the water availability initially increases

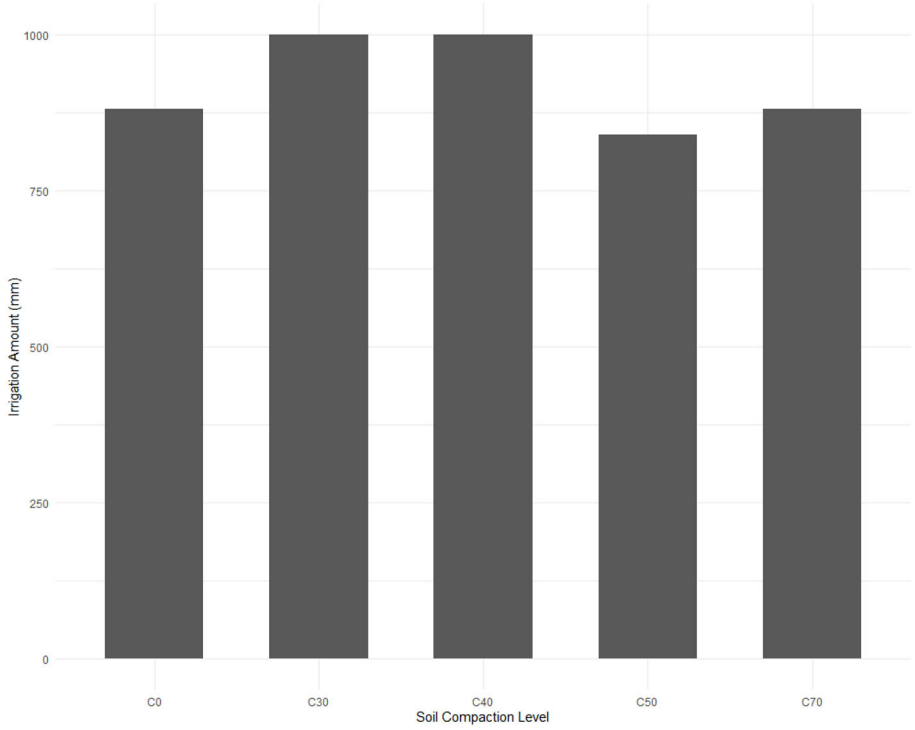

FIGURE 11
Irrigation amount for the five compaction levels over the 153 days.

with increased compaction due to an increase in water retention capacity. When soil compaction reaches a certain level, the soil particles become densely packed, which limits the infiltration of water and causes a significant decline in water availability.

For the modeling of the case study with HYDRUS1-D, we used Durner's dual porosity model by implementing the bimodal parameters of the constrained VG model since the software version does not have the unconstrained bimodal VG model. When considering some scenarios, the soil matric potential in conjunction with water content helps us to understand the water availability (WA) and then calculate the required irrigation. The SMP indicates the water comfort range of potatoes, and the soil water data shows what changes are occurring in the soil due to daily water absorption and indicates the amount of water required to maintain the root zone at an optimal level.

For the same SMP, the unsaturated K increases because we have more micropore for the same level of compaction. We also have an increase in soil water retention, which means that the soil can hold onto more water, but this water may not be easily available to plant roots. The potatoes started to stress, even though the soil was still quite wet, although there is water available in the soil, it cannot flow to the roots of the plants.

The moderate compaction levels provide a beneficial plant-soil water regime through increased soil particle contact and water retention, reducing moisture loss (Brown and Hoxie, 1998). As a result, when the irrigation amount is increased on a compacted soil, the water may not be able to penetrate the soil quickly enough to be absorbed by the plant roots, leading to water wastage and a decrease in irrigation efficiency. The decrease in irrigation amount with compaction is due to the reduction in soil hydraulic conductivity, which leads to reduced infiltration rates and water availability for plant uptake. These results provide both indications of the hydraulic behavior of compacted soils and irrigation management.

6. Summary and conclusions

In this study, simplified evaporation tests were conducted on loamy sand soil planted with potato (Goldrush species) with different soil bulk densities to investigate the effect of compaction on the hydraulic properties.

Based on the experimental results, following conclusions can be obtained:

(1) The simplified evaporation and dew point methods described adequately the soil hydraulic characteristic curves.
(2) The independent measurements of Ks are important.
(3) Compaction had a clear effect on SWRC.
(4) The dual-porosity soil model was used to evaluate the SWRC parameters. The van Genuchten PDI-bimodal SWRC (VGm b-PDI) was adopted to compare and discuss the effect of compaction. This dual porosity behavior includes the existence of distinct but interacting macro and microporous regions. The calibration of the n values of the SWRC curves for non-compacted C0 soils was required.
(5) For SHCC, the model revealed a change from the van Genchuten bimodal to unimodal distribution but also more with those predicted by PDI. However, the changes in the

SHCC were noticed after forcing the hydraulic conductivity values. With the use of the calibrated Ks, the statistical analysis improved.

(6) The optimization of the specific soil hydraulic parameters for the compaction levels has shown that determining the precise irrigation volume for each level can be an effective irrigation practice.

(7) Soil compaction can significantly affect the availability of water to potatoes through irrigation. In fact, the irrigation amount decreases with compaction.

(8) At a moderate compaction level (C40), the irrigation amount for potato cultivation was optimal.

Overall, the combined methodology of HYPROP and HYDRUS 1D contribute to an excellent soil description of compacted soil hydrology, therefore, we recommend testing a wide range of soil types with different compaction levels.

Data availability statement

The original contributions presented in the study are included in the article/supplementary material, further inquiries can be directed to the corresponding author.

Author contributions

YM: Formal analysis, Methodology, Software, Writing—original draft. SG: Formal analysis, Project administration, Supervision, Validation, Writing—review and editing. PC: Supervision, Validation, Writing—review and editing. JB: Writing—review and editing.

Conflict of interest

The authors declare that the research was conducted in the absence of any commercial or financial relationships that could be construed as a potential conflict of interest.

Publisher's note

All claims expressed in this article are solely those of the authors and do not necessarily represent those of their affiliated organizations, or those of the publisher, the editors and the reviewers. Any product that may be evaluated in this article, or claim that may be made by its manufacturer, is not guaranteed or endorsed by the publisher.

References

Alaoui, A., Lipiec, J., and Gerke, H. H. (2011). A review of the changes in the soil pore system due to soil deformation : a hydrodynamic perspective. *Soil Till. Res.* 115-116, 1–15. doi: 10.1016/j.still.2011.06.002

Assouline, S., and Or, D. (2014). The concept of field capacity revisited: defining intrinsic static and dynamic criteria for soil internal drainage dynamics. *Water Resour. Res.* 50, 4787–4802. doi: 10.1002/2014WR015475

Balaine, N., Clough, T. J., Beare, M. H., Thomas, S. M., and Meenken, E. D. (2016). Soil gas diffusivity controls N_2O and N_2 emissions and their ratio. *Soil Sci. Soc. Am. J.* 80, 529–540. doi: 10.2136/sssaj2015.09.0350

Brooks, R., and Corey, T. (1964). Hydraulic properties of porous media and their relation to drainage design. *Trans. ASAE* 26-28. doi: 10.13031/2013.40684

Brown, J. S. H., and Hoxie, F. E. (1998). Encyclopedia of North American Indians. *J. Am. Hist.* 85, 203. doi: 10.2307/2568455

CEAEQ (2003). *Méthode d'analyse. Détermination de la matière organique par incinération: Méthode de perte au feu (PAF)*. Centre d'expertise en analyse environnementale du Québec. MA. 1010 – PAF 1.0, 9. Available online at: http://collections.banq.qc.ca/ark:/52327/bs35531 (accessed February 12, 2023).

Doorenbos, J., Kassam, A. H., Bentvelsen, C., and Uittenbogaard, G. (1979). "Yield response to water 11 This paper is a summary of: Doorenbos, J., A. H. Kassam, C. Bentvelsen, V. Branscheid, M. Smith, J. Plusje, G. Uittenbogaard and H. van der Wal; Yield response to water, FAO irrigation and drainage paper," in *Irrigation and Agricultural Development*, ed S. S. JOHL (Pergamon), 257–280.

Doorenbos, J., and Pruitt, W. O. (1977). *Crop Water Requirements. FAO Irrigation and Drainage Paper 24.* Rome: FAO, 144.

Farquharson, R., and Baldock, J. (2008). Concepts in modelling N2O emissions from land use. *Plant Soil* 309, 147–167. doi: 10.1007/s11104-007-9485-0

Filipović, V., Defterdarović, J., Krevh, V., Filipović, L., Ondrašek, G., Kranjčec, F., et al. (2021). Estimation of stagnosol hydraulic properties and water flow using uni- and bimodal porosity models in erosion-affected hillslope vineyard soils. *Agronomy* 12, 33. doi: 10.3390/agronomy12010033

Fox, J., and Weisberg, S. (2020). *An R Companion to Applied Regression, 3rd Edn.* Sage. Available online at: https://r-forge.r-project.org/projects/car/ (accessed August 06, 2022).

Fredlund, D. G., and Xing, A. (1994). Equations for the soil-water characteristic curve. *Can. Geotech. J.* 31, 521–532. doi: 10.1139/t94-061

Gerke, H. H., and van Genuchten, M. T. (1993). A dual-porosity model for simulating the preferential movement of water and solutes in structured porous media. *Water Resour. Res.* 29, 305–319. doi: 10.1029/92WR02339

Haghverdi, A., Najarchi, M., Öztürk, H. S., and Durner, W. (2020). Studying unimodal, bimodal, PDI and bimodal-PDI variants of multiple soil water retention models : I. direct model fit using the extended evaporation and dewpoint methods. *Water* 12, 900. doi: 10.3390/w12030900

Hansson, L. J., Koestel, J., Ring, E., and Gärdenäs, A. I. (2018). Impacts of off-road traffic on soil physical properties of forest clear-cuts : X-ray and laboratory analysis. *Scand. J. For. Res.* 33, 166–177. doi: 10.1080/02827581.2017.1339121

Hill, J. N. S., and Sumner, M. E. (1967). Effect of bulk density on moisture characteristics of soils. *Soil Sci.* 103, 234–238. doi: 10.1097/00010694-196704000-00002

IA (2005). *Landscape IrrigationScheduling and Water Management.* Available online at: https://www.researchgate.net/publication/242476742_Smart_Irrigation_Controllers_Operation_of_Evapotranspiration-Based_Controllers1 (accessed August 20, 2022).

Jabro, J. D., Allen, B. L., Rand, T., Dangi, S. R., and Campbell, J. W. (2021). Effect of previous crop roots on soil compaction in 2 yr rotations under a no-tillage system. *Land* 10, 202. doi: 10.3390/land10020202

Kirkham, M. B. (2005). "Chapter 8 - Field capacity, wilting point, available water, and the non-limiting water range," in *Principles of Soil and Plant Water Relations*, ed M. B. Kirkham (Academic Press), 101–115. doi: 10.1016/B978-012409751-3/50008-6

Kosugi, K. (1996). Lognormal distribution model for unsaturated soil hydraulic properties. *Water Resour. Res.* 32, 2697–2703. doi: 10.1029/96WR01776

Kuang, X., Jiao, J. J., Shan, J., and Yang, Z. (2021). A modification to the van Genuchten model for improved prediction of relative hydraulic conductivity of unsaturated soils. *Eur. J. Soil Sci.* 72, 1354–1372. doi: 10.1111/ejss.13034

Lehmann, P., Assouline, S., and Or, D. (2008). Characteristic lengths affecting evaporative drying of porous media. *Phys. Rev. E* 77, 056309. doi: 10.1103/PhysRevE.77.056309

Lipovetsky, T., Zhuang, L., Teixeira, W. G., Boyd, A., May Pontedeiro, E., Moriconi, L., et al. (2020). HYPROP measurements of the unsaturated hydraulic properties of a carbonate rock sample. *J. Hydrol.* 591, 125706. doi: 10.1016/j.jhydrol.2020.125706

Maas, E. V., and Hoffman, G. J. (1977). Crop salt tolerance-current assessment. *J. Irrigat. Drain. Div.* 103, 115–134. doi: 10.1061/JRCEA4.0001137

Matteau, J.-P., Célicourt, P., Létourneau, G., Gumiere, T., and Gumiere, S. J. (2021). Potato varieties response to soil matric potential based irrigation. *Agronomy* 11, 352. doi: 10.3390/agronomy11020352

Matthews, G. P., Laudone, G. M., Gregory, A. S., Bird, N. R. A., de Matthews, A. G., and Whalley, W. R. (2010). Measurement and simulation of the effect of compaction on the pore structure and saturated hydraulic conductivity of grassland and arable soil : effect of compaction on structure and co. *Water Resour. Res.* 46. doi: 10.1029/2009WR007720

Mendiburu, F. D. (2019). *Agricolae: Statistical Procedures for Agricultural Research*. R Package version 1.3-1. Available online at: https://CRAN.R-project.org/package=agricolae (accessed August 20, 2022)

METER Group (2023). *Examining Plant Stress Using Water Potential and Hydraulic Conductivity*. Available online at: https://www.metergroup.com/en/meter-environment/case-studies/examining-plant-stress-using-water-potential-and-hydraulic (accessed August 2, 2022).

Meurer, K., Barron, J., Chenu, C., Coucheney, E., Fielding, M., Hallett, P., et al. (2020). A framework for modelling soil structure dynamics induced by biological activity. *Glob. Chang. Biol.* 26, 5382–5403. doi: 10.1111/gcb.15289

Millington, R. J., and Quirk, J. P. (1961). Permeability of porous solids. *Transact. Farad. Soc.* 57, 1200. doi: 10.1039/tf9615701200

Mooney, S. J., and Nipattasuk, W. (2006). Quantification of the effects of soil compaction on water flow using dye tracers and image analysis. *Soil Use Manag.* 19, 356–363. doi: 10.1111/j.1475-2743.2003.tb00326.x

Mossadeghi-Björklund, M., Arvidsson, J., Keller, T., Koestel, J., Lamandé, M., Larsbo, M., et al. (2016). Effects of subsoil compaction on hydraulic properties and preferential flow in a Swedish clay soil. *Soil Till. Res.* 156, 91–98. doi: 10.1016/j.still.2015.09.013

Mossadeghi-Björklund, M., Jarvis, N., Larsbo, M., Forkman, J., and Keller, T. (2019). Effects of compaction on soil hydraulic properties, penetration resistance and water flow patterns at the soil profile scale. *Soil Use Manag.* 35, 367–377. doi: 10.1111/sum.12481

Nawaz, M. F., Bourri,é, G., and Trolard, F. (2013). Soil compaction impact and modelling. A review. *Agron. Sustain. Dev.* 33, 291–309. doi: 10.1007/s13593-011-0071-8

Parvin, N., Beckers, E., Plougonven, E., Léonard, A., and Degré, A. (2017). Dynamic of soil drying close to saturation : What can we learn from a comparison between X-ray computed microtomography and the evaporation method? *Geoderma* 302, 66–75. doi: 10.1016/j.geoderma.2017.04.027

Penman (1940a). Gas and vapor movements in the soil. I. The diffusion of vapors through porous solids. *J. Agr. Sci.* 30, 437–462. doi: 10.1017/S0021859600048164

Penman (1940b). Gas and vapor movements in the soil. II. The diffusion of carbon dioxide through porous solids. *J. Agr. Sci.* 30, 570–581. doi: 10.1017/S0021859600048231

Pertassek, T., Peters, A., and Durner, W. (2015). *HYPROP-FIT Software User's Manual, V.3.0*. München: UMS GmbH, 66.

Peters, A. (2013). Simple consistent models for water retention and hydraulic conductivity in the complete moisture range : hydraulic models for the complete moisture range. *Water Resour. Res.* 49, 6765–6780. doi: 10.1002/wrcr.20548

Peters, A., Iden, S. C., and Durner, W. (2015). Revisiting the simplified evaporation method : Identification of hydraulic functions considering vapor, film and corner flow. *J. Hydrol.* 527, 531–542. doi: 10.1016/j.jhydrol.2015.05.020

R Core Team (2019). *R: A Language and Environment for Statistical Computing*. Available online at: https://www.r-project.org/ (accessed April 17, 2020).

Reynolds, W. D., and Elrick, D. E. (2002). "Constant head soil core (tank) method," in *Methods of Soil Analysis. Part 4. SSSA Book Ser.5*, eds J. H. Dane, and G. C. Topp (Madison, WI: SSSA), 804–808.

Richard, G., Cousin, I., Sillon, J. F., Bruand, A., and Guérif, J. (2001). Effect of compaction on the porosity of a silty soil : Influence on unsaturated hydraulic properties: Soil compaction, pore geometry and hydraulic properties. *Eur. J. Soil Sci.* 52, 49–58. doi: 10.1046/j.1365-2389.2001.00357.x

Rudiyanto, M. B., Shah, R. M., Setiawan, B. I., and van Genuchten, M. (2020). Simple functions for describing soil water retention and the unsaturated hydraulic conductivity from saturation to complete dryness. *J. Hydrol.* 588, 125041. doi: 10.1016/j.jhydrol.2020.125041

Schelle, H., Heise, L., Jänicke, K., and Durner, W. (2013). Water retention characteristics of soils over the whole moisture range : a comparison of laboratory methods: water retention characteristics. *Eur. J. Soil Sci.* 64, 814–821. doi: 10.1111/ejss.12108

Schelle, H., Iden, S. C., Peters, A., and Durner, W. (2010). Analysis of the agreement of soil hydraulic properties obtained from multistep-outflow and evaporation methods. *Vadose Zone J.* 9, 1080–1091. doi: 10.2136/vzj2010.0050

Schnider, U. (1980). Ein Schnellverfahren zur Messung der Wasserleitfähigkeit im teilgesättigten Boden an Stechzylinderproben. *Archiv Acker Pflanzenbau Bodenkunde* 24, 1–7.

Sidhu, D., and Duiker, S. W. (2006). Soil compaction in conservation tillage : crop impacts. *Agron. J.* 98, 1257–1264. doi: 10.2134/agronj2006.0070

Šimunek, J., Genuchten, M., and Šejna, M. (2016). Recent developments and applications of the HYDRUS computer software packages. *Vadose Zone J.* 15, 1–25. doi: 10.2136/vzj2016.04.0033

Smith, C. W., Johnston, M. A., and Lorentz, S. A. (2001). The effect of soil compaction on the water retention characteristics of soils in forest plantations. *South Afr. J. Plant ad Soil* 18, 87–97. doi: 10.1080/02571862.2001.10634410

van Genuchten, M. (1980). A closed-form equation for predicting the hydraulic conductivity of unsaturated soils. *Soil Sci. Soc. Am. J.* 44, 892–898. doi: 10.2136/sssaj1980.03615995004400050002x

Wind, G. P. (1968). "Capillary conductivity data estimated by a simple method," in *Symposium on Water in the Unsaturated Zone (IASH/AIHS-Unesco)*, eds R.E. Rijtema, and H. Wassink, 181–191. Available online at: https://unesdoc.unesco.org/ark:/48223/pf0000014319.locale$=$en (accessed January 15, 2023).

Zhai, Q., and Rahardjo, H. (2015). Estimation of permeability function from the soil–water characteristic curve. *Eng. Geol.* 199, 148–156. doi: 10.1016/j.enggeo.2015.11.001

Zhang, S., Grip, H., and Lövdahl, L. (2006). Effect of soil compaction on hydraulic properties of two loess soils in China. *Soil Till. Res.* 90, 117–125. doi: 10.1016/j.still.2005.08.012

Zhuang, L., Bezerra Coelho, C. R., Hassanizadeh, S. M., and van Genuchten, M. (2017). Analysis of the hysteretic hydraulic properties of unsaturated soil. *Vadose Zone J.* 16, vzj2016.11.0115. doi: 10.2136/vzj2016.11.0115